

Photochemical Upconversion Theory: Importance of Triplet Energy Levels and Triplet Quenching

David Jefferies,¹ Timothy W. Schmidt,² and Laszlo Frazer^{1,*}

¹ARC Centre of Excellence in Exciton Science, School of Chemistry, Monash University, Clayton, Victoria, Australia

²ARC Centre of Excellence in Exciton Science, School of Chemistry, University of New South Wales Sydney, Sydney, New South Wales, Australia



(Received 10 April 2019; revised manuscript received 14 May 2019; published 13 August 2019)

Photochemical upconversion is a promising way to boost the efficiency of solar cells using triplet-exciton annihilation. Currently, predicting the performance of photochemical upconversion devices is challenging. We present an open-source software package that takes experimental parameters as inputs and gives the figure of merit of an upconversion system, enabling theory-driven design of better solar-energy devices. We incorporate the statistical distribution of triplet excitons between the sensitizer and the emitter. Using the dynamic quenching effect of the sensitizer on emitter triplet excitons, we show that the optimal sensitizer concentration can be below the sensitizer solubility limit in liquid devices. These theoretical contributions can explain, without the use of heavy-atom-induced triplet-exciton formation or phenyl-group rotation, the experimental failure of zinc octaethylporphyrin to effectively sensitize diphenylanthracene, where platinum octaethylporphyrin succeeds. Our predictions indicate a change in direction for device design that will reduce triplet-exciton losses.

DOI: 10.1103/PhysRevApplied.12.024023

I. INTRODUCTION

Solar cells have a transparent region below their band gap. The transparent region plays an important role in limiting the efficiency of conventional solar cells illuminated by sunlight [1,2]. Photochemical upconversion is a phenomenon that converts light a solar cell cannot use into light that the cell can use [3–9]. The utility comes from the spontaneous increase in the energy per photon. Owing to its exothermic nature, photochemical upconversion can be relatively efficient [10–12].

Photochemical upconversion transfers energy through a series of energy levels, which are illustrated by the energy-level diagram in Fig. 1. The energy levels are in two different molecules, the sensitizer [10,13–17] and the emitter [18–22]. First, sunlight is absorbed by the sensitizer molecules. Second, the sensitizer undergoes intersystem crossing, which produces a triplet exciton. Third, the sensitizer molecule transfers energy to an emitter molecule [23,24]. The triplet-exciton state of the emitter is relatively long lived [21,25], enabling energy to be stored for conversion. Fourth, emitter excitons undergo triplet annihilation. Triplet annihilation converts a pair of triplet excitons to one singlet exciton. Fifth, the emitter molecules in the singlet excited state produce fluorescence. This fluorescence

has a higher energy per photon than the light that was absorbed in the first step, so it can be used by a solar cell.

Photochemical upconversion cannot exceed 50% quantum yield because triplet annihilation converts two triplet excitons into one singlet exciton [26]. A quantum yield of 50% is highly advantageous, because upconversion enables the use of a region of the solar spectrum where the solar-cell external quantum efficiency is zero [27]. In addition, the output quanta have more energy than the input quanta; the energy efficiency exceeds the quantum yield.

In upconversion devices, the balance between desirable triplet-exciton annihilation and other forms of triplet loss determines the quantum yield of upconversion [23]. Here, we use simulations [4] to show how advanced triplet-exciton physics can be applied to shift the fate of excitons toward annihilation and away from other decay mechanisms. In particular, we focus on the Boltzmann distribution of triplets between molecules and the recently discovered quenching action of the sensitizer [25,28] on the triplet-exciton storage in the emitter.

II. OVERVIEW OF CALCULATIONS

We calculate the accepted figure of merit for photochemical upconversion, which is the photocurrent per unit area caused by upconversion, under the assumption that the solar cell has perfect quantum efficiency [29]. As illustrated in Fig. 2, we simulate a device consisting of a

*laszlo@laszlofrazer.com

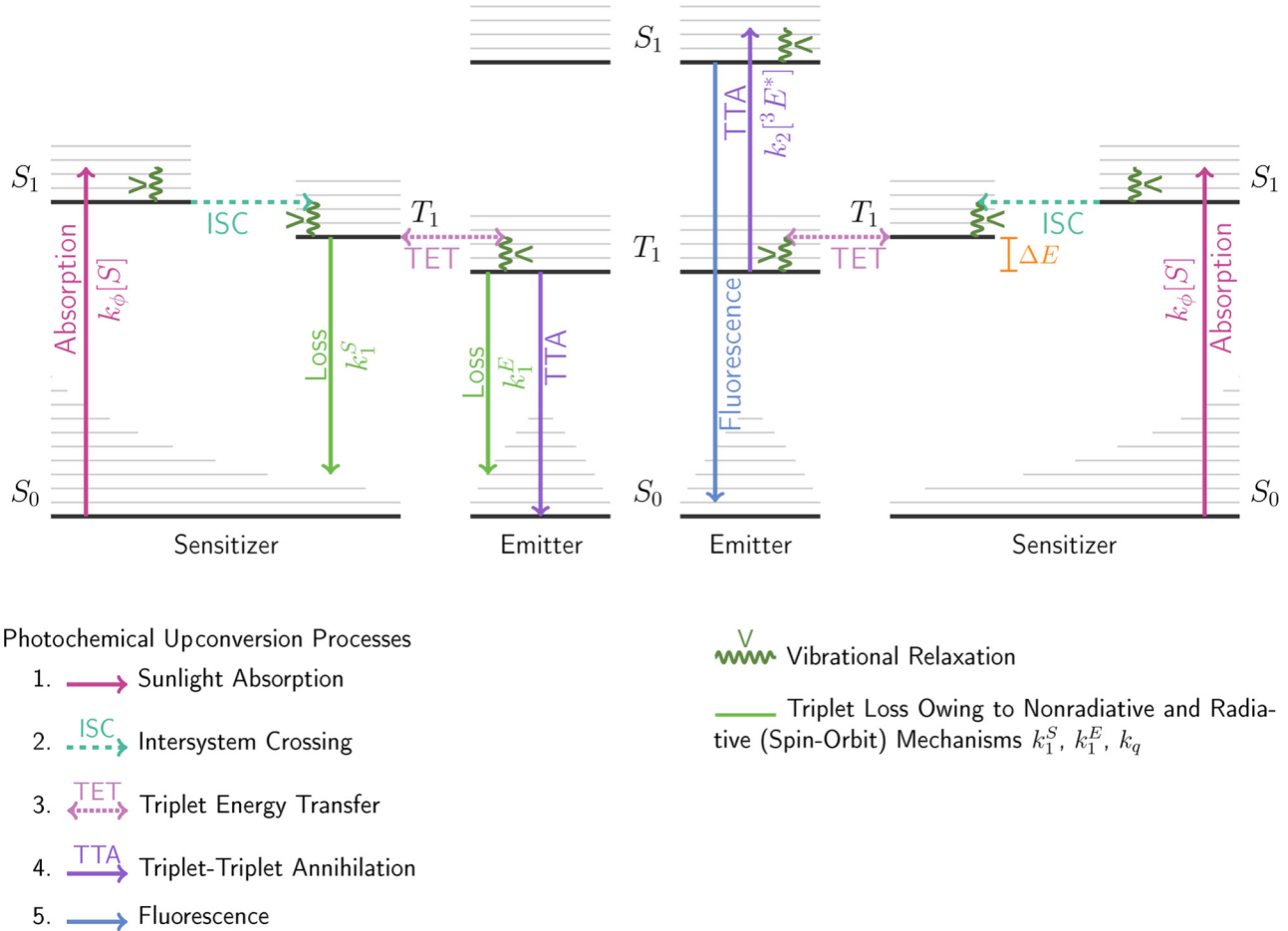


FIG. 1. A photochemical upconversion energy-level diagram. The system consists of sensitizer and emitter molecules. The sensitizer molecules capture light and transfer the resulting exciton to the emitter. S_n and T_n indicate the n th singlet and triplet spin energy levels, respectively. The triplet energy transfer double-ended arrows indicate that rapid triplet energy transfer achieves an equilibrium, rather than complete transfer. Figure adapted from Ref. [25].

solar cell, an anabathmophore layer that performs photochemical upconversion [11], and a Lambertian diffuse reflector [4]. Our simulations use random samples from the AM1.5G solar spectrum. For each sunlight sample, we use random sampling to determine whether the light is absorbed by the solar cell, absorbed by the sensitizer, or diffusely reflected.

It is established that, in well-constructed systems, the sensitizer intersystem crossing, triplet energy transfer [21,25,30–34], and fluorescence have negligible losses. Therefore, we assume that they are perfectly efficient. While our methods can be adapted to poorly constructed systems, including low intersystem crossing rates, triplet transfer rates, and fluorescence yields, these possibilities are beyond the scope of this report. Triplet energy transfer is further discussed in Sec. III.

The quantum yield of photochemical upconversion Φ_{UC} is computed according to the accepted theory [23], which incorporates the triplet-exciton annihilation rate constant k_2 , the triplet-exciton concentration [T], and the regular

triplet-loss rate constant k_1 :

$$\Phi_{UC} = \frac{k_2[T]}{2(k_1 + k_2[T])}. \quad (1)$$

This yield determines the quantity of fluorescence.

Using random samples from the fluorescence spectrum, we calculate the rate at which fluorescence is absorbed by the solar cell. The figure of merit is calculated from this rate. We also include the self-absorption and photon recycling [35], owing to both the sensitizer and the emitter, including diffuse reflections from the bottom surface of the anabathmophore. Self-absorption is typically small for well-designed systems.

Our simulations use experimental solar-spectral irradiance, sensitizer absorption, emitter absorption, and emitter emission spectra. Therefore, they are readily adapted to a wide range of illumination conditions and chemistries. For this paper, we use the sensitizer

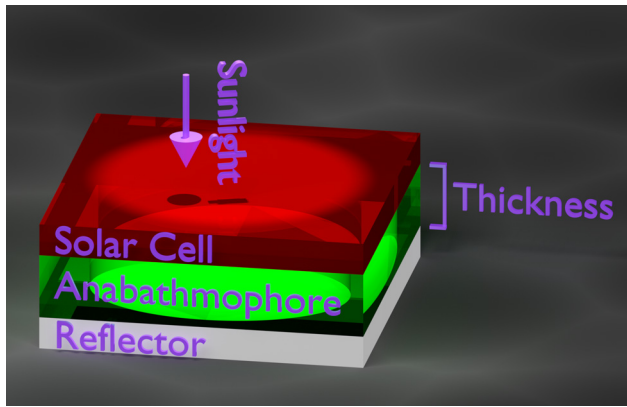


FIG. 2. An illustration of the device, including the solar cell, the light upconverting anabathmophore, and the light-distributing diffuse reflector. The anabathmophore upconverts the light that is not absorbed by the solar cell owing to the band gap. The sensitizer and emitter are located in the anabathmophore.

zinc octaethylporphyrin and the emitter diphenylanthracene. Previous work has investigated the relationship between the chemical structure and upconversion properties of closely related sensitizers [16,18,21,25,36–39] and emitters [21,22,40–43]. The chemical structures are illustrated in Fig. 3 and the spectra are presented in Fig. 4. For the solar cell, we use the Tauc model of direct band-gap absorption so that the band gap of the solar cell is a free variable [44,45]. Details of the algorithm are in Sec. V.

III. TRIPLET KINETICS OWING TO TRIPLET ENERGY LEVELS

The rate of energy transfer from the sensitizer to the emitter is much faster than the triplet decay rate of the

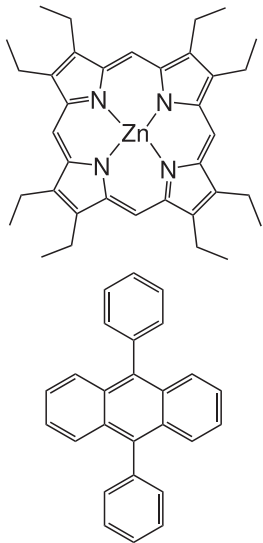


FIG. 3. The molecular structures of the sensitizer zinc octaethylporphyrin (top) and the emitter 9,10-diphenylanthracene (bottom).

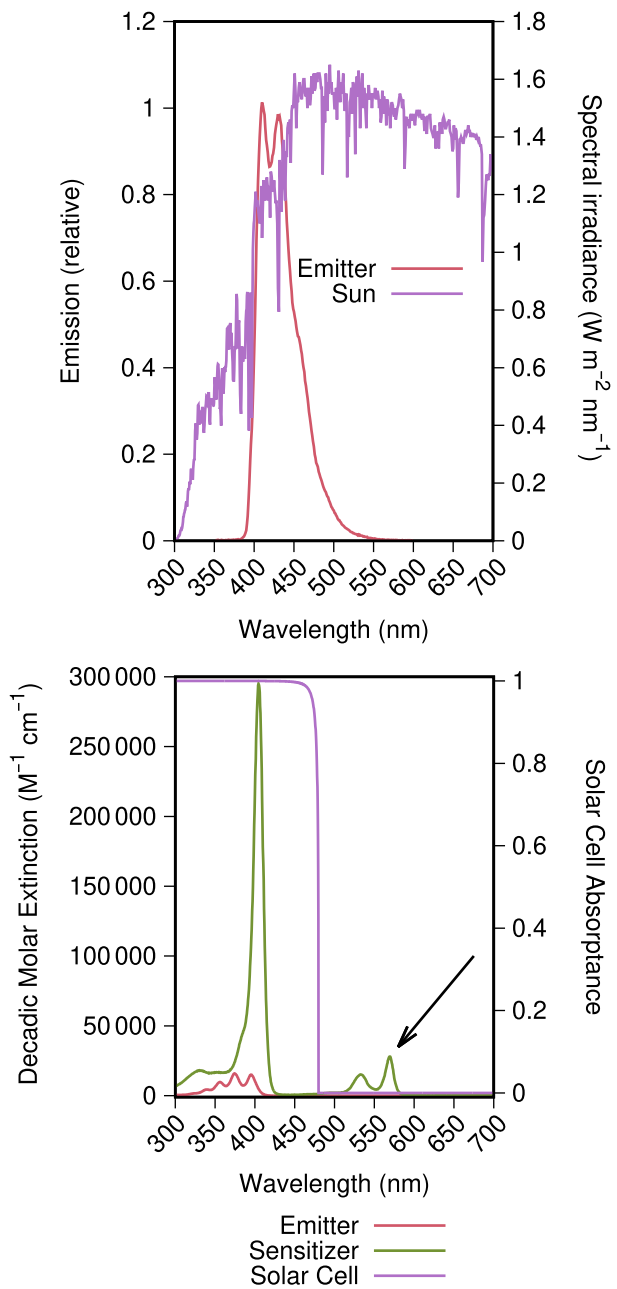


FIG. 4. Example spectra. Top: the solar-spectral irradiance and the diphenylanthracene emitter fluorescence (normalized to peak). Bottom: the solar-cell absorptance (with a band gap at 480 nm), the zinc-octaethylporphyrin-sensitizer molar extinction, and the emitter molar extinction. The arrow indicates the absorption peaks that sensitize upconversion. Since the solar cell is simulated as a single interface, it has a dimensionless absorptance [46].

sensitizer [21,25,30–34]. As a result, it is common to discuss the decay rate of triplet excitons (excluding annihilation) k_1 as if it were the same as the triplet decay rate of the emitter. However, we will show that the sensitizer triplet decay rate can play an important role in determining

TABLE I. Physical rate constants assumed in the simulation.

Name	Symbol	Compound	Value	Reference(s)
Triplet decay of sensitizer	k_1^S	Zinc octaethylporphyrin	8550 s^{-1}	[21]
Triplet decay of emitter, $[S] = 0$	k_1^0	Diphenylanthracene	2000 s^{-1}	[25]
Quenching	k_q	Both	$4.8 \times 10^7 \text{ M}^{-1} \text{ s}^{-1}$ $8.0 \times 10^{-14} \text{ cm}^3 \text{ s}^{-1}$	[25]
Triplet annihilation	k_2	Diphenylanthracene	$2.8 \times 10^9 \text{ M}^{-1} \text{ s}^{-1}$ $4.7 \times 10^{-12} \text{ cm}^3 \text{ s}^{-1}$	[21, 40]

the figure of merit, even though energy transfer is faster than triplet decay.

In equilibrium, the distribution of triplets between the sensitizer and the emitter is according to the Boltzmann distribution [47]. Experiments show that the triplet energy transfer is the fastest rate when the emitter concentration is high [21]. We assume that the sensitizer and emitter triplet-exciton populations are in equilibrium. The equilibrium is illustrated in Fig. 1 by the triplet-energy-transfer arrows from the sensitizer to the emitter and from the emitter to the sensitizer.

If k_1^S is the triplet-decay rate constant in the sensitizer [21], k_1^E is the triplet-decay rate constant in the emitter [25], $[S]$ is the sensitizer concentration, $[E]$ is the emitter concentration, k_B is the Boltzmann constant, T is the temperature, and ΔE is the difference between the sensitizer triplet energy level and the emitter triplet energy level, then the overall triplet decay rate is as follows:

$$k_1 = \frac{[S]k_1^S e^{-(\Delta E/k_B T)} + [E]k_1^E}{[S]e^{-(\Delta E/k_B T)} + [E]} \quad (2)$$

The rate constants are listed in Table I [21, 25].

As shown in Fig. 5, if $\Delta E > 0$, then as the temperature increases, k_1 increases, which leads to a reduced quantum yield. This result emphasizes that the interplay between environmental conditions, such as heating by the sun and cooling by the wind [48], with the exothermic nature of upconversion must be considered when designing an energy conversion system.

In order to generate triplet excitons, the sensitizer must have a high intersystem crossing rate. As a result, the sensitizer's triplet-decay rate constant k_1^S is relatively large [21, 49, 50]. However, device designers have the freedom to select an emitter molecule with a small triplet-decay rate constant k_1^E . Equations (1) and (2) show that a large k_1^S decreases the quantum yield.

In addition, a pair of triplet states located in the sensitizer typically cannot produce upconversion because known sensitizer molecules lack a suitable first excited singlet spin state [51]. It is possible to harvest higher excited states [52], a phenomenon that we do not simulate. While annihilation of triplet excitons located in different molecules can be efficient [53], we assume that sensitizers

will not have this property. Therefore, the concentration of *usable* triplet excitons is as follows:

$$[^3E^*] = [T] \frac{[E]}{[S]e^{-(\Delta E/k_B T)} + [E]} \quad (3)$$

ΔE is the energy lost during transfer of a triplet exciton from the sensitizer to the emitter. It is indicated in Fig. 1. The quantum yield is more precisely written as follows:

$$\Phi_{UC} = \frac{k_2[^3E^*]}{2(k_1 + k_2[^3E^*])} \quad (4)$$

In many cases, ΔE much is larger than the thermal energy. Then, it is not necessary to consider k_1^S . An excessively large ΔE is detrimental to energy efficiency because it

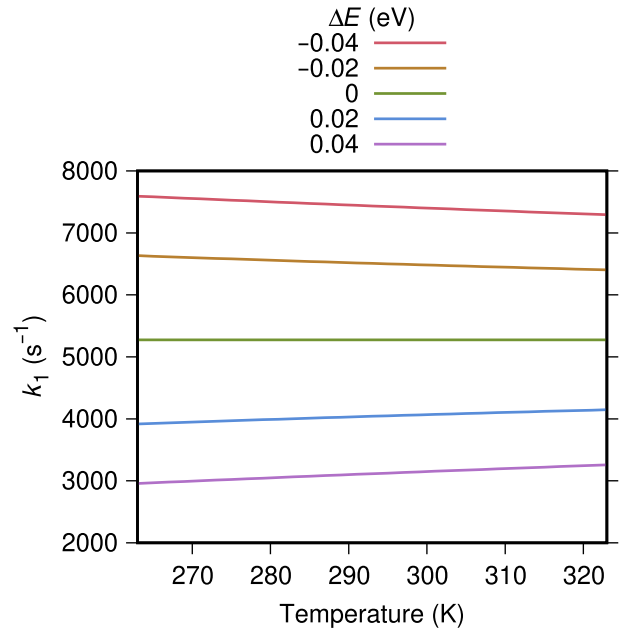


FIG. 5. k_1 as a function of the temperature for several values of ΔE according to the statistical distribution of triplet excitons. A smaller k_1 leads to a better Φ_{UC} [Eq. (1)]. Better upconversion systems are exothermic ($\Delta E \gg k_B T$), so their k_1 increases when heated by sunlight. Despite the detrimental effect of heating, exothermic systems remain superior. For this figure, we use $[S] = [E] = 1 \text{ mM}$.

reduces the upward shift in the energy of the upconverted photons. If ΔE is enhanced by shifting the sensitizer triplet energy upward, then the portion of the solar spectrum that could be captured by the sensitizer will decrease. If ΔE is enhanced by shifting the emitter triplet energy downward, it may be necessary to also shift the fluorescence energy downward to keep the system exothermic. This leads to the necessity of selecting a solar cell with a smaller band gap. The solar cell will then block more light from reaching the sensitizer.

If ΔE is negative, it is possible to increase the photon energy by more than a factor of 2 [47]. However, more triplet excitons will be distributed in the sensitizer molecules, which makes the quantum yield small.

Figure 6 shows the simulated figure of merit, the current density, as a function of the emitter concentration. For low values of ΔE , a high ratio of emitter molecules to sensitizer molecules is needed to produce upconversion. An abundance of emitter molecules ensures that some triplet excitons are distributed to the emitter. If ΔE is large, then the Boltzmann distribution ensures that triplet excitons are located in the emitter molecules even if those molecules are scarce. We do not include the additional decrease in

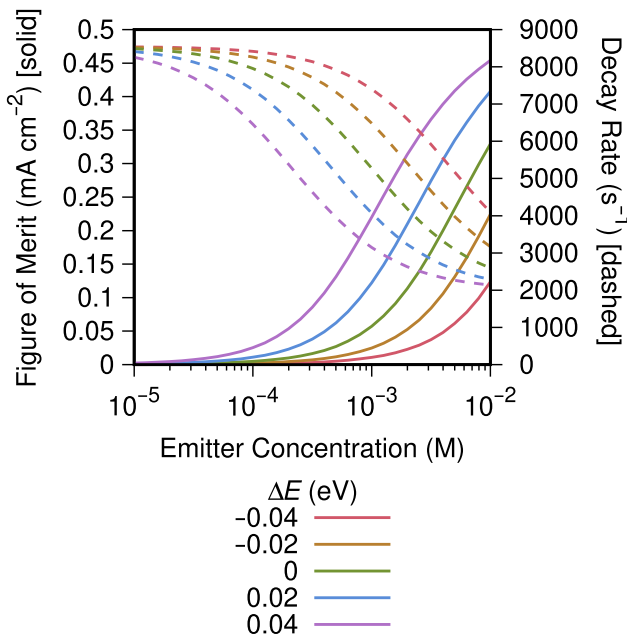


FIG. 6. The triplet-decay rate constant k_1 (dashed curves) and figure of merit (solid curves) as a function of the emitter concentration $[E]$ for several values of ΔE . The sensitizer concentration is 1 mM, the temperature is 300 K, and the anabathmophore thickness is 0.1 cm. If ΔE or $[E]$ are not big enough, upconversion becomes inefficient because triplets decay in the sensitizer. A large triplet energy transfer rate cannot overcome this decay. In addition, triplet excitons in the sensitizer are not available for upconversion.

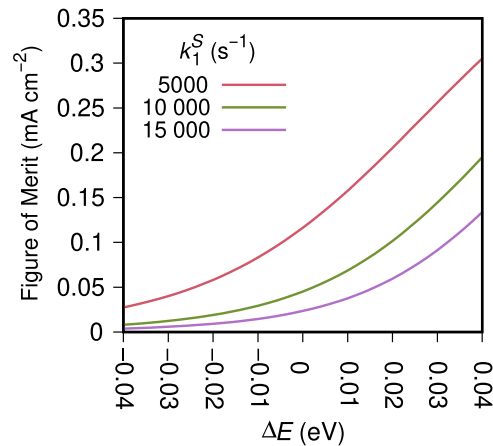


FIG. 7. The figure of merit as a function of the difference in the triplet energy levels, ΔE , for a variety of sensitizer triplet-decay rate constants, k_1^S , and an anabathmophore thickness of 0.1 cm. Energy losses owing to k_1^S are mitigated if $\Delta E \gg k_B T$. Platinum octaethylporphyrin with diphenylanthracene exhibits this advantage. Zinc octaethylporphyrin does not. However, the spectral shift achieved by upconversion decreases as ΔE increases. For this figure, we use $[S] = [E] = 1$ mM.

the figure of merit that occurs at very low emitter concentrations. Decrease may occur because the triplet excitons do not reach the equilibrium distribution before decaying or the emitter becomes saturated with excitations.

Figure 7 shows that upconversion fails to produce photocurrent when all the triplet decay occurs in the sensitizer, because $\Delta E \ll 0$. A smaller sensitizer triplet decay k_1^S makes the figure of merit more sensitive to ΔE near $\Delta E = 0$. The zinc-octaethylporphyrin-diphenylanthracene system is in this region. Both ΔE and k_1^S can contribute to controlling triplet-exciton loss.

IV. DYNAMIC TRIPLET QUENCHING CAUSED BY SENSITIZER

The sensitizer concentration determines the excitation density [54]. A high excitation density produces efficient annihilation because the triplet concentration is in the numerator of Eq. (4). Therefore, one would expect that the highest achievable sensitizer concentration will produce the highest possible upconversion figure of merit. We have recently shown that k_1^E , the triplet decay in the emitter, is dependent on the sensitizer concentration [25]. Here, we show the resulting impact on the figure of merit and the device design.

A. Model

The decay rate of triplets in the emitter in the absence of sensitizer and excluding annihilation is k_1^0 , which typically ranges from 10^2 to 10^4 s^{-1} [25]. The rate constant quantifying the emitter-triplet quenching by the sensitizer, k_q , is

typically less than $5 \times 10^7 \text{ M}^{-1} \text{s}^{-1}$ [25]. The total triplet losses in the emitter are as follows:

$$k_1^E = k_1^0 + k_q[S]. \quad (5)$$

The solubility limit on $[S]$ is above 1 mM [25].

B. Quenching reduces the figure of merit

Figure 8 shows the calculated figure of merit with and without the quenching constant. Here, we assume strongly exothermic triplet energy transfer. The device thickness, which is important to achieving a high triplet concentration [4], is also included as a variable. Without the quenching constant, the figure of merit increases with the concentration. The optimal device thickness decreases with the concentration, as the absorption length decreases. With the inclusion of a quenching constant, a maximum figure of merit exists below a sensitizer concentration of 10^{-4} M .

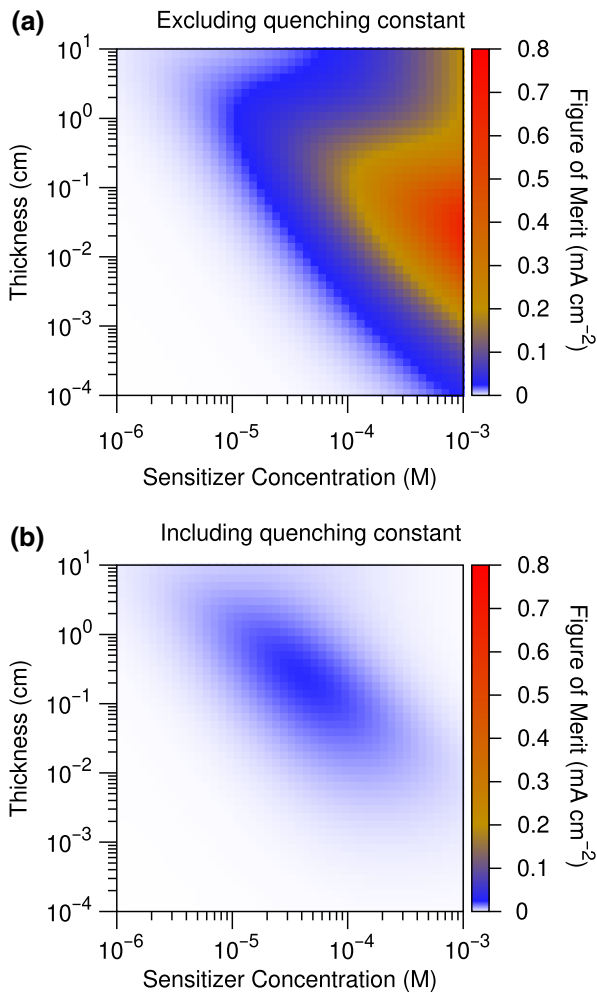


FIG. 8. The figure of merit as a function of the sensitizer concentration and thickness, (a) without and (b) with the quenching constant $k_q = 4.8 \times 10^7 \text{ M}^{-1} \text{s}^{-1}$ [25]. White indicates a zero figure of merit. We assume that $\Delta E = 0.3 \text{ eV}$.

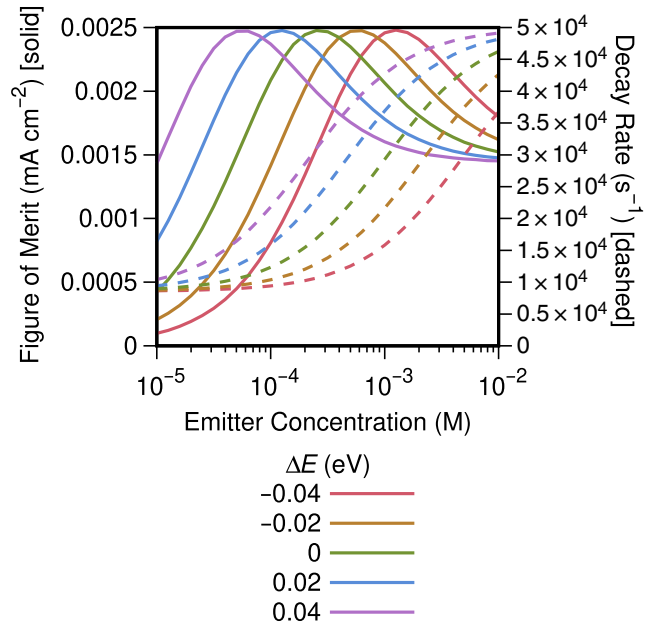


FIG. 9. The triplet-decay rate constant k_1 (dashed curves) and the figure of merit (solid curves) as a function of the emitter concentration for several values of ΔE with a quenching constant of $4.8 \times 10^7 \text{ M}^{-1} \text{s}^{-1}$. The sensitizer concentration is 1 mM, the temperature is 300 K, and the thickness is 0.1 cm. Compared to Fig. 6, the figure of merit is reduced by the quenching action of the sensitizer. The figure of merit has a maximum for the same reason.

The relationship between the figure of merit and the emitter concentration is dramatically changed by the inclusion of the quenching constant. In our model, the triplet excitons in the sensitizer are protected from concentration-dependent quenching. As a result, in Fig. 9, the triplet decay rate k_1 increases with the emitter concentration. Unlike the results in Fig. 6, which exclude quenching, the figure of merit has a maximum with respect to the emitter concentration when quenching is included. We omit the concentration quenching of triplet excitons within triplet sensitizers, which can be approximately $10^7 \text{ M}^{-1} \text{s}^{-1}$, and may be important [55,56].

C. Interplay of sensitizer quenching and Boltzmann statistics

The quenching effect of Eq. (5) was experimentally demonstrated in situations where $\Delta E \gg k_B T$ [25]. As the sensitizer concentration increased, k_1 increased in a linear fashion. If analysis including Eq. (5) is performed on a system that is not strongly exothermic, then the contribution of Boltzmann statistics from Eq. (2) will cause the quenching constant to be overestimated. For zinc octaethylporphyrin and diphenylanthracene, the reported ΔE is 0.02 eV [21,57–60]. In our view, the experimental and theoretical uncertainty on this value is sufficient for the sign to be uncertain.

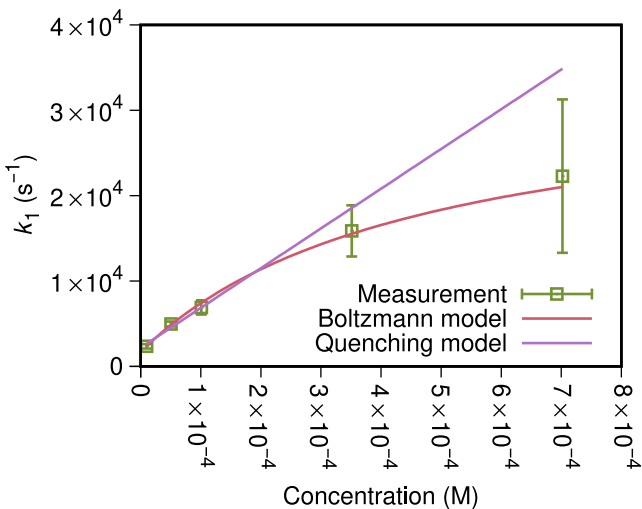


FIG. 10. The experimental triplet decay rate in the emitter as a function of the sensitizer concentration. The linear quenching model (5) is compared against the Boltzmann model including Eqs. (2) and (5). The downward curvature of the data suggests that some triplet excitons remain in the sensitizer after the triplet energy transfer reaches equilibrium. Data from Ref. [25].

In Fig. 10, we reanalyze the zinc octaethylporphyrin and diphenylanthracene data from Ref. [25]. We compare the prediction of Eq. (5) with the combined prediction of Eqs. (2) and (5). Equation (2) increases the number of free parameters, so its inclusion must improve the accuracy of the model. While the experimental uncertainty is sufficiently large that neither model can be rejected, it does seem that ΔE is not large enough to keep all the triplet excitons in the emitter. We suggest that $\Delta E = -0.02 \pm 0.01$ eV. The triplet energy transfer may be endothermic.

If the mechanism giving rise to k_q were an external heavy-atom effect, then it should increase with the atomic number Z . However, the opposite was observed [25]. Zinc-containing sensitizer ($Z = 30$) had the highest k_q , but palladium ($Z = 46$) and platinum ($Z = 78$) were similar to each other. The inclusion of ΔE in the theory opens up the possibility that zinc-containing sensitizer does not really have a higher k_q . Both parameters can explain the experimental increase in the emitter triplet-exciton decay. Future measurements over a range of emitter concentrations will eliminate this ambiguity. ΔE and k_q provide theoretical explanations of the relationship between the atomic number and the upconversion performance that do not require models based on phenyl-group rotation [21]. Table II shows that both ΔE and k_q can change the figure of merit, but that k_q is more important.

D. Selecting the optimal design

Figure 11 gives the optimized figure of merit as a function of the quenching constant. This shows the harmful effect of the sensitizer quenching the emitter on device

TABLE II. The figure of merit J_{UC} under different assumptions about ΔE and k_q . The sensitizer concentration and device thickness are optimized separately for each calculation. With no k_q , the sensitizer concentration is constrained to 1 mM by solubility.

ΔE (eV)	k_q ($M^{-1} s^{-1}$)	J_{UC} ($\mu A cm^{-2}$)
-0.02	4.8×10^7	23.5(1)
-0.02	0	370.0(5)
0.3	4.8×10^7	24.2(1)
0.3	0	673.2(1)

performance. In addition, k_q makes it necessary to increase the device thickness and decrease the sensitizer concentration to generate the most current from an upconversion device. The quantity of sensitizer used may be important as far as cost effectiveness is concerned.

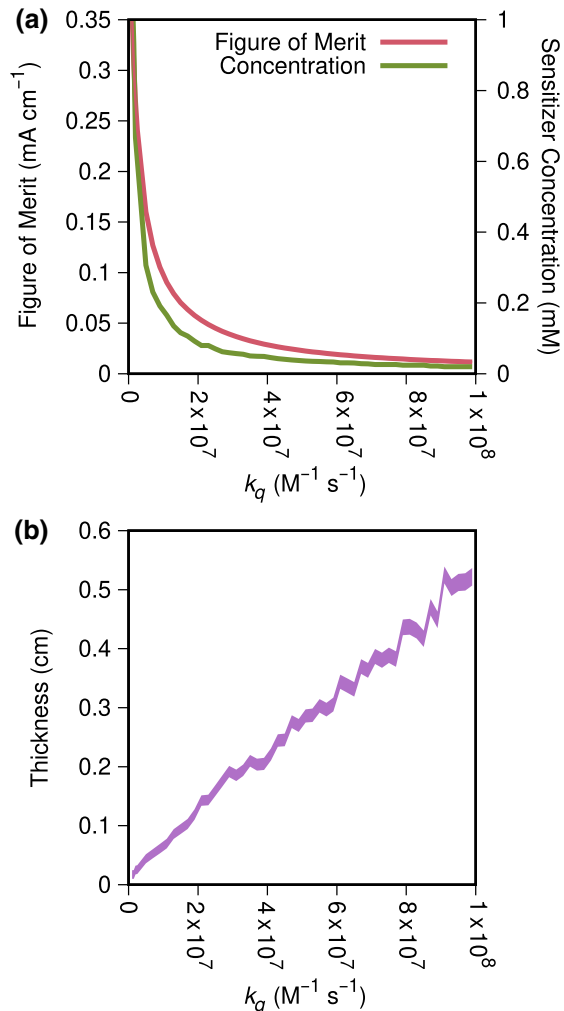


FIG. 11. (a) The maximum figure of merit and the optimal sensitizer concentration as a function of the quenching constant. (b) The optimal thickness as a function of the quenching constant. We assume that $\Delta E = 0$ and $[E] = 10 \times 10^{-2}$ M. The width of the purple curve indicates the estimated Monte Carlo error.

V. FIGURE-OF-MERIT ALGORITHM

A. Sampling sunlight

The device is modeled as an infinite plane with the sunlight incident perpendicular to the surface. The solar spectral irradiance is stochastically sampled 10^9 times using the cumulative distribution function of the AM1.5G spectrum. To determine whether a sample is absorbed into the solar cell, the Tauc model of direct band-gap semiconductors [44,45] is scaled so that there is a 99% probability of the solar cell absorbing the sample 0.1 eV above the 2.6 eV band gap. If the sample is not absorbed, it is assumed to reach the anabathmophore. Refractive-index matching is assumed throughout the simulation.

B. Light transmission and scattering

The interior of the anabathmophore is divided into 10^5 bins, arranged vertically. The bins are used to model the inhomogeneous distribution of excitons within the anabathmophore.

If a sample reaches the anabathmophore, spline interpolation is used to calculate the absolute value of the corresponding sensitizer and the emitter molar absorptivities from the experimental spectra shown in Fig. 4. The emitter absorption spectrum is filtered so that any molar extinction below $1000 \text{ M}^{-1} \text{ cm}^{-1}$ is set to $0 \text{ M}^{-1} \text{ cm}^{-1}$, to mitigate instrument noise. This reduces nonphysical anti-Stokes shifts. Using the sum of the molar absorptivities, the distance traveled by the sample is stochastically determined from the Beer-Lambert law [54]. The concentrations and molar absorptivities are used to stochastically assign the sample to be absorbed by the sensitizer or emitter. The distance traveled determines the bin at which the sample is absorbed. For each bin, the number of samples absorbed and reabsorbed by the sensitizer and the emitter are recorded.

If the distance traveled exceeds the thickness of the anabathmophore, Lambertian reflection is simulated and the distance traveled is recalculated. The upward component of the distance traveled is used to determine the bin. If the distance traveled upward goes beyond the region occupied by the anabathmophore, the sample is not absorbed by the anabathmophore and does not contribute to the figure of merit.

C. Sampling fluorescence

Samples absorbed by the sensitizer and emitter are modeled separately and have different fluorescence yields. For sensitizer excitation, we assume that the singlet yield of triplet annihilation is perfect [26,61]. The quantum yield Φ_{UC} is calculated using Eq. (4), with values from Table I. The temperature is assumed to be 300 K. Since the triplet energy transfer is rapid [21], it is assumed to be in equilibrium. The triplet concentration is calculated as

follows [23]:

$$[T] = \frac{-k_1 + \sqrt{k_1^2 + 4k_\phi k_2[S]}}{2k_2}, \quad (6)$$

where k_ϕ is the excitation rate, computed under the usual assumption that the irradiance of the sun is 1 kW m^{-2} . The upconversion yield Φ_{UC} is different for each bin because k_ϕ is different. Samples absorbed by the emitter have a perfect fluorescence yield, corresponding to an assumption of a perfect fluorescence quantum yield. The quantum-yield assumption also applies to converted triplet excitons.

To simulate emission, fluorescence samples generated according to the quantum yield are each stochastically assigned a wavelength. The wavelength is determined using the cumulative distribution function of the experimental emitter fluorescence spectrum in Fig. 4. The fluorescence is propagated in a random direction from the middle of the bin according to the Beer-Lambert law. If the direction of travel is downward, the sample can undergo Lambertian reflection. The vertical component of the distance traveled determines the bin into which the sample is reabsorbed. If the sample escapes from the top of the anabathmophore, the Tauc model is reused to determine whether the solar cell has absorbed the sample [44,45]. If it has, then the sample contributes to the figure of merit.

Reabsorption and emission are recalculated five times to account for photon recycling [35]. During each cycle, the number of samples reabsorbed in each bin and Φ_{UC} are recalculated. Typically, reabsorption is small. Here, we choose a sensitizer that is mostly transparent to fluorescence; our previous results suggest that molar extinction is more important to the figure of merit than reduced reabsorption, so it is important to account for photon recycling [4].

D. Figure of merit

The total radiant exposure entering the system is calculated by summing the photon energies of samples stochastically generated from the solar spectrum. The radiant exposure is then divided by the standard solar irradiance, 1 kW m^{-2} , to find the simulation duration t . The figure of merit, the current density, is

$$\frac{en}{t} \quad (7)$$

where e is the fundamental charge and n is the area density of the emitter fluorescence samples absorbed by the solar cell.

VI. CONCLUSIONS

Previously, we have argued that 0.1 mA m^{-2} is a meaningful figure of merit [4]. Reaching this goal requires

improvement. The efficiency of photochemical upconversion relies on the exothermic nature of each process involved in the steps of light conversion. Here, we relate a decrease in the potential energy that drives triplet energy transfer to a reduction in the figure of merit. We quantitatively demonstrate that the photocurrent is improved when the energy loss $\Delta E \gg k_B T$. The quenching of triplets located in the emitter but caused by the sensitizer also inhibits the figure of merit, even when exothermic operation is successfully achieved. In the future, upconversion can be advanced by creating sensitizer-emitter pairs that have a large ΔE and a small quenching k_q .

The poor performance of zinc octaethylporphyrin with diphenylanthracene, compared to alternative sensitizers paired with diphenylanthracene, can be explained by the quenching action of the sensitizer on the emitter and the alignment of the triplet energy levels. These properties cannot be determined by only measuring triplet-energy-transfer rate constants. The Boltzmann distribution of triplet excitons inhibits upconversion even when energy transfer is efficient.

Our results highlight the value of measuring triplet decay rates as a function of concentrations. This type of experiment provides information about exciton conversion processes that lead to major changes in the figure of merit. When $\Delta E \approx 0$, theoretical and phosphorescence methods may not be precise enough. In addition, a pulsed experiment showing a high triplet-energy transfer rate is not sufficient to show complete triplet transfer in equilibrium. If the Boltzmann factor is in doubt, then both the sensitizer and emitter concentration should be explored to find ΔE and k_q .

The simulation program, which is available from Ref. [62], can readily be used to predict the relative merits of different compounds with respect to their usefulness as sensitizers and emitters. This is particularly useful for the search for sensitizers that have absorption spectra that efficiently capture sunlight. In addition, different solar-cell band gaps, illumination conditions, and rate constants can be conveniently modeled. The manual is included as Supplemental Material [63].

We show that, using knowledge of the sensitizer and emitter physics, the energy conversion performance of complete devices can be simulated. These simulations enable prediction of the best device design without requiring the construction of many devices with different molecular concentrations and device geometries.

ACKNOWLEDGMENTS

This work was supported by the Australian Research Council Centre of Excellence in Exciton Science (Grant No. CE170100026). D.J. acknowledges a ResearchFirst fellowship from Monash University. This research was

undertaken with the assistance of resources and services from the National Computational Infrastructure (NCI), which is supported by the Australian Government. We thank Elham Gholizadeh and Rowan MacQueen for the experimental spectra used in this work.

- [1] W. Shockley and H. J. Queisser, Detailed balance limit of efficiency of *p-n* junction solar cells, *J. Appl. Phys.* **32**, 510 (1961).
- [2] L. C. Hirst and N. J. Ekins-Daukes, Fundamental losses in solar cells, *Progr. Photovoltaics: Res. Appl.* **19**, 286 (2011).
- [3] J. Pedrini and A. Monguzzi, Recent advances in the application triplet-triplet annihilation-based photon upconversion systems to solar technologies, *J. Photon. Energy* **8**, 022005 (2017).
- [4] L. Frazer, J. K. Gallaher, and T. Schmidt, Optimizing the efficiency of solar photon upconversion, *ACS Energy Lett.* **2**, 1346 (2017).
- [5] Y. Zeng, J. Chen, T. Yu, G. Yang, and Y. Li, Molecular-supramolecular light harvesting for photochemical energy conversion: Making every photon count, *ACS Energy Lett.* **2**, 357 (2017).
- [6] T. F. Schulze and T. W. Schmidt, Photochemical upconversion: Present status and prospects for its application to solar energy conversion, *Energy Environ. Sci.* **8**, 103 (2015).
- [7] C. E. McCusker and F. N. Castellano, Materials integrating photochemical upconversion, *Top. Curr. Chem.* **374**, 19 (2016).
- [8] V. Gray, K. Moth-Poulsen, B. Albinsson, and M. Abrahamsson, Towards efficient solid-state triplet-triplet annihilation based photon upconversion: Supramolecular, macromolecular and self-assembled systems, *Coord. Chem. Rev.* **362**, 54 (2018).
- [9] E. Y. Chen, C. Milleville, J. M. Zide, M. F. Doty, and J. Zhang, Upconversion of low-energy photons in semiconductor nanostructures for solar energy harvesting, *MRS Energy Sustainability* **5**, e16 (2018).
- [10] M. Wu, D. N. Congreve, M. W. Wilson, J. Jean, N. Geva, M. Welborn, T. Van Voorhis, V. Bulović, M. G. Bawendi, and M. A. Baldo, Solid-state infrared-to-visible upconversion sensitized by colloidal nanocrystals, *Nat. Photonics* **10**, 31 (2016).
- [11] L. Frazer, Photochemical upconversion light emitting diode (LED): Theory of triplet annihilation enhanced by a cavity, *Adv. Theory Simul.* **2**, 1800099 (2019).
- [12] M. A. Baldo, C. Adachi, and S. R. Forrest, Transient analysis of organic electrophosphorescence, II. Transient analysis of triplet-triplet annihilation, *Phys. Rev. B* **62**, 10967 (2000).
- [13] T. C. Wu, D. N. Congreve, and M. A. Baldo, Solid state photon upconversion utilizing thermally activated delayed fluorescence molecules as triplet sensitizer, *Appl. Phys. Lett.* **107**, 031103 (2015).
- [14] K. Okumura, K. Mase, N. Yanai, and N. Kimizuka, Employing core-shell quantum dots as triplet sensitizers for photon upconversion, *Chem. A Eur. J.* **22**, 7721 (2016).

- [15] S. Amemori, N. Yanai, and N. Kimizuka, Metallonaphthalocyanines as triplet sensitizers for near-infrared photon upconversion beyond 850 nm, *Phys. Chem. Chem. Phys.* **17**, 22557 (2015).
- [16] S. Baluschev, V. Yakutkin, G. Wegner, T. Miteva, G. Nelles, A. Yasuda, S. Chernov, S. Aleshchenkov, and A. Cheprakov, Upconversion with ultrabroad excitation band: Simultaneous use of two sensitizers, *Appl. Phys. Lett.* **90**, 181103 (2007).
- [17] Z. Huang, X. Li, M. Mahboub, K. M. Hanson, V. M. Nichols, H. Le, M. L. Tang, and C. J. Bardeen, Hybrid molecule-nanocrystal photon upconversion across the visible and near-infrared, *Nano Lett.* **15**, 5552 (2015).
- [18] A. Turshatov, D. Busko, Y. Avlasevich, T. Miteva, K. Landfester, and S. Baluschev, Synergetic effect in triplet-triplet annihilation upconversion: Highly efficient multi-chromophore emitter, *ChemPhysChem* **13**, 3112 (2012).
- [19] X. Yu, X. Cao, X. Chen, N. Ayres, and P. Zhang, Triplet-triplet annihilation upconversion from rationally designed polymeric emitters with tunable inter-chromophore distances, *Chem. Commun.* **51**, 588 (2015).
- [20] J. K. H. Pun, J. K. Gallaher, L. Frazer, S. K. Prasad, C. B. Dover, R. W. MacQueen, and T. W. Schmidt, TIPS-anthracene: A singlet fission or triplet fusion material? *J. Photon. Energy* **8**, 022006 (2018).
- [21] V. Gray, A. Dreos, P. Erhart, B. Albinsson, K. Moth-Poulsen, and M. Abrahamsson, Loss channels in triplet-triplet annihilation photon upconversion: Importance of annihilator singlet and triplet surface shapes, *Phys. Chem. Chem. Phys.* **19**, 10931 (2017).
- [22] C. Gao, J. Y. Seow, B. Zhang, C. Hall, A. Tilley, J. White, T. Smith, and W. W. H. Wong, Tetraphenylethene 9, 10-diphenylanthracene derivatives—synthesis and photophysical properties, *ChemPlusChem* **84**, 746 (2019).
- [23] T. W. Schmidt and F. N. Castellano, Photochemical upconversion: The primacy of kinetics, *J. Phys. Chem. Lett.* **5**, 4062 (2014).
- [24] Y. Y. Cheng, A. Nattestad, T. F. Schulze, R. W. MacQueen, B. Fückel, K. Lips, G. G. Wallace, T. Khoury, M. J. Crossley, and T. W. Schmidt, Increased upconversion performance for thin film solar cells: A trimolecular composition, *Chem. Sci.* **7**, 559 (2016).
- [25] E. M. Gholizadeh, L. Frazer, R. W. MacQueen, J. K. Gallaher, and T. W. Schmidt, Photochemical upconversion is suppressed by high concentrations of molecular sensitizers, *Phys. Chem. Chem. Phys.* **20**, 19500 (2018).
- [26] Y. Y. Cheng, B. Fückel, T. Khoury, R. G. Clady, M. J. Tayebjee, N. Ekins-Daukes, M. J. Crossley, and T. W. Schmidt, Kinetic analysis of photochemical upconversion by triplet-triplet annihilation: Beyond any spin statistical limit, *J. Phys. Chem. Lett.* **1**, 1795 (2010).
- [27] M. J. Tayebjee, D. R. McCamey, and T. W. Schmidt, Beyond Shockley-Queisser: Molecular approaches to high-efficiency photovoltaics, *J. Phys. Chem. Lett.* **6**, 2367 (2015).
- [28] T. W. Schmidt and R. W. MacQueen, in *Proceedings of SPIE* (SPIE, San Diego, CA, 2015), Vol. 9562, p. 956202.
- [29] Y. Y. Cheng, B. Fückel, R. W. MacQueen, T. Khoury, R. G. Clady, T. F. Schulze, N. Ekins-Daukes, M. J. Crossley, B. Stannowski, K. Lips, *et al.*, Improving the light-harvesting of amorphous silicon solar cells with photochemical upconversion, *Energy Environ. Sci.* **5**, 6953 (2012).
- [30] A. Monguzzi, R. Tubino, and F. Meinardi, Upconversion-induced delayed fluorescence in multicomponent organic systems: Role of Dexter energy transfer, *Phys. Rev. B* **77**, 155122 (2008).
- [31] Z. Huang, Z. Xu, M. Mahboub, X. Li, J. W. Taylor, W. H. Harman, T. Lian, and M. L. Tang, PbS/CdS core-shell quantum dots suppress charge transfer and enhance triplet transfer, *Angew. Chem. Int. Ed.* **56**, 16583 (2017).
- [32] R. Younts, H.-S. Duan, B. Gautam, B. Saparov, J. Liu, C. Mongin, F. N. Castellano, D. B. Mitzi, and K. Gundogdu, Efficient generation of long-lived triplet excitons in 2D hybrid perovskite, *Adv. Mater.* **29**, 1604278 (2017).
- [33] L. Nienhaus, M. Wu, N. Geva, J. J. Shepherd, M. W. Wilson, V. Bulović, T. Van Voorhis, M. A. Baldo, and M. G. Bawendi, Speed limit for triplet-exciton transfer in solid-state PbS nanocrystal-sensitized photon upconversion, *ACS Nano* **11**, 7848 (2017).
- [34] T. N. Singh-Rachford and F. N. Castellano, Triplet sensitized red-to-blue photon upconversion, *J. Phys. Chem. Lett.* **1**, 195 (2009).
- [35] L. M. Pazos-Outón, M. Szumilo, R. Lamboll, J. M. Richter, M. Crespo-Quesada, M. Abdi-Jalebi, H. J. Beeson, M. Vrućinić, M. Alsari, H. J. Snaith, *et al.*, Photon recycling in lead iodide perovskite solar cells, *Science* **351**, 1430 (2016).
- [36] Y. V. Aulin, M. van Sebille, M. Moes, and F. C. Grozema, Photochemical upconversion in metal-based octaethyl porphyrin-diphenylanthracene systems, *RSC Adv.* **5**, 107896 (2015).
- [37] F. Deng, A. Francis, W. Weare, and F. Castellano, Photochemical upconversion and triplet annihilation limit from a boron dipyrromethene emitter, *Photochem. Photobiol. Sci.* **14**, 1265 (2015).
- [38] B. Wang, B. Sun, X. Wang, C. Ye, P. Ding, Z. Liang, Z. Chen, X. Tao, and L. Wu, Efficient triplet sensitizers of palladium (II) tetraphenylporphyrins for upconversion-powered photoelectrochemistry, *J. Phys. Chem. C* **118**, 1417 (2014).
- [39] Z. Xun, Y. Zeng, J. Chen, T. Yu, X. Zhang, G. Yang, and Y. Li, Pd-porphyrin oligomers sensitized for green-to-blue photon upconversion: The more the better? *Chem. A Eur. J.* **22**, 8654 (2016).
- [40] V. Gray, D. Dzebo, A. Lundin, J. Alborzpour, M. Abrahamsson, B. Albinsson, and K. Moth-Poulsen, Photophysical characterization of the 9,10-disubstituted anthracene chromophore and its applications in triplet-triplet annihilation photon upconversion, *J. Mater. Chem. C* **3**, 11111 (2015).
- [41] V. Gray, K. Börjesson, D. Dzebo, M. Abrahamsson, B. Albinsson, and K. Moth-Poulsen, Porphyrin-anthracene complexes: Potential in triplet-triplet annihilation upconversion, *J. Phys. Chem. C* **120**, 19018 (2016).
- [42] S. Baluschev, V. Yakutkin, T. Miteva, G. Wegner, T. Roberts, G. Nelles, A. Yasuda, S. Chernov, S. Aleshchenkov, and A. Cheprakov, A general approach for

- non-coherently excited annihilation up-conversion: Transforming the solar-spectrum, *New J. Phys.* **10**, 013007 (2008).
- [43] M. B. Smith and J. Michl, Singlet fission, *Chem. Rev.* **110**, 6891 (2010).
- [44] B. D. Viezbicke, S. Patel, B. E. Davis, and D. P. Birnie III, Evaluation of the Tauc method for optical absorption edge determination: ZnO thin films as a model system, *Phys. Status Solidi (b)* **252**, 1700 (2015).
- [45] J. Tauc, Optical properties and electronic structure of amorphous Ge and Si, *Mater. Res. Bull.* **3**, 37 (1968).
- [46] A. D. McNaught, *Compendium of Chemical Terminology* (IUPAC, Research Triangle Park, USA, 2014). 2nd ed.
- [47] Y. Y. Cheng, B. Fückel, T. Khouri, R. G. Clady, N. Ekins-Daukes, M. J. Crossley, and T. W. Schmidt, Entropically driven photochemical upconversion, *J. Phys. Chem. A* **115**, 1047 (2011).
- [48] E. Skoplaki and J. A. Palyvos, On the temperature dependence of photovoltaic module electrical performance: A review of efficiency/power correlations, *Solar Energy* **83**, 614 (2009).
- [49] S. Perun, J. Tatchen, and C. M. Marian, Singlet and triplet excited states and intersystem crossing in free-base porphyrin: TDDFT and DFT/MRCI study, *ChemPhysChem* **9**, 282 (2008).
- [50] C. Mongin, S. Garakyaragh, N. Razgoniaeva, M. Zamkov, and F. N. Castellano, Direct observation of triplet energy transfer from semiconductor nanocrystals, *Science* **351**, 369 (2016).
- [51] M. Kasha, Characterization of electronic transitions in complex molecules, *Discuss. Faraday Soc.* **9**, 14 (1950).
- [52] H. Goudarzi, S. Limbu, J. Cabanillas-Gonzalez, V. M. Zenonos, J.-S. Kim, and P. E. Keivanidis, Impact of molecular conformation on triplet-fusion induced photon energy up-conversion in the absence of exothermic triplet energy transfer, *J. Mater. Chem. C* **7**, 3634 (2019).
- [53] X. Cao, B. Hu, and P. Zhang, High upconversion efficiency from hetero triplet-triplet annihilation in multiacceptor systems, *J. Phys. Chem. Lett.* **4**, 2334 (2013).
- [54] D. Swinehart, The Beer-Lambert law, *J. Chem. Educ.* **39**, 333 (1962).
- [55] J. B. Callis, J. M. Knowles, and M. Gouterman, Porphyrins, XXVI. Triplet excimer quenching of free base, zinc, palladium, and platinum complexes, *J. Phys. Chem.* **77**, 154 (1973).
- [56] D. Dexter and J. H. Schulman, Theory of concentration quenching in inorganic phosphors, *J. Chem. Phys.* **22**, 1063 (1954).
- [57] O. Ohno, Y. Kaizu, and H. Kobayashi, Luminescence of some metalloporphyrins including the complexes of the IIIb metal group, *J. Chem. Phys.* **82**, 1779 (1985).
- [58] G.-Z. Wu, W.-X. Gan, and H.-K. Leung, Photophysical properties of meso-substituted octaethylporphyrines and their zinc complexes, *J. Chem. Soc. Faraday Trans.* **87**, 2933 (1991).
- [59] X. Liu, E. K. Yeow, S. Velate, and R. P. Steer, Photophysics and spectroscopy of the higher electronic states of zinc metalloporphyrins: A theoretical and experimental study, *Phys. Chem. Chem. Phys.* **8**, 1298 (2006).
- [60] J. Brinen and J. Koren, The lowest triplet state of 9, 10 diphenylanthracene, *Chem. Phys. Lett.* **2**, 671 (1968).
- [61] S. Hoseinkhani, R. Tubino, F. Meinardi, and A. Monguzzi, Achieving the photon up-conversion thermodynamic yield upper limit by sensitized triplet-triplet annihilation, *Phys. Chem. Chem. Phys.* **17**, 4020 (2015).
- [62] <http://laszlofrazer.com>
- [63] See the Supplemental Material at <http://link.aps.org/supplemental/10.1103/PhysRevApplied.12.024023> for the manual for the upconversion solar-cell simulator.